

Background Entropic Expansion Metric (BEEM)

Biswajit De

06 Sep 2025

1 Introduction & Motivation

The standard cosmological model, Λ CDM, has achieved remarkable success across an impressive dynamic range of observations: the acoustic peaks of the cosmic microwave background (CMB), the late-time clustering of galaxies, and the distance-redshift relation from Type Ia supernovae (SNe Ia) and baryon acoustic oscillations (BAO). Despite the successes, as the theory evolved over time we found anomalies like those described below, which motivate testing the model's assumptions and seeking complementary frameworks.

1.1 Cosmological Context and Open Questions

Λ CDM — a spatially flat FRW background with cold dark matter (CDM) and a cosmological constant Λ — accounts for the key observables with a minimal parameter set. Nonetheless, several persistent puzzles have emerged:

- The **Hubble tension**: local measurements of H_0 differ from CMB-inferred values by more than 5σ .
- **Low-redshift growth anomalies**: mild but recurrent hints of suppressed or enhanced clustering amplitudes, e.g. the S_8 tension.
- **Conceptual questions**: the nature of Λ , the “why now” problem, and the absence of a microphysical mechanism for cosmic acceleration.

These motivate exploration of frameworks that preserve interpretability, are falsifiable, and can absorb new data without ad hoc fine-tuning.

1.2 Concept of a Background Entropic Expansion Metric (BEEM)

We introduce **BEEM** — **Background Entropic Expansion Metric** — a phenomenological extension that re-expresses cosmological distances in terms of a lattice-like, time-evolving effective metric. Key principles include:

1. **Homogeneity and isotropy preserved**: BEEM modifies the background expansion, not the perturbation sector.
2. **Lattice field interpretation**: the cosmic scale factor is replaced by a reconfiguration field whose growth reflects the microscopic “lattice” of spacetime evolving toward equilibrium.
3. **Entropic expansion**: the field evolves so as to maximize entropy, providing a natural explanation for cosmic acceleration without invoking an arbitrary constant Λ term.

When the field is static, BEEM reduces exactly to Λ CDM distances. When it evolves, it induces smooth, testable deviations in D_M , D_H , and D_V across redshift.

1.3 Motivating BEEM through Observational Tensions

Recent low-redshift surveys have revealed mild but systematic tensions in isotropic BAO distance ratios (notably near $z \approx 0.1$) and occasional preference for evolving $w(z)$ models in joint SN+BAO analyses. BEEM provides a natural and testable proposal: in other words, the mysterious Λ term may not be required at all, since BEEM demonstrates that cosmic acceleration can emerge as a natural consequence of the background lattice reconfiguring itself to maximize entropy. This framework allows us to diagnose whether observed anomalies indicate:

- a genuine departure from Λ CDM geometry, or
- a localized outlier or systematic (e.g. BAO branch choice).

1.4 BEEM–Inflation: Extending to the Primordial Epoch

To remain consistent with CMB–inferred early–time physics, BEEM is embedded in a two–branch history:

1. **Early branch (inflation):** a rapid exponential growth of the lattice field sets the primordial sound horizon r_s and seeds structure formation.
2. **Late branch (BEEM):** a slower, possibly evolving lattice reconfiguration governs low– z distances.

A smooth matching at reheating ensures continuity of aH and preserves the acoustic scale.

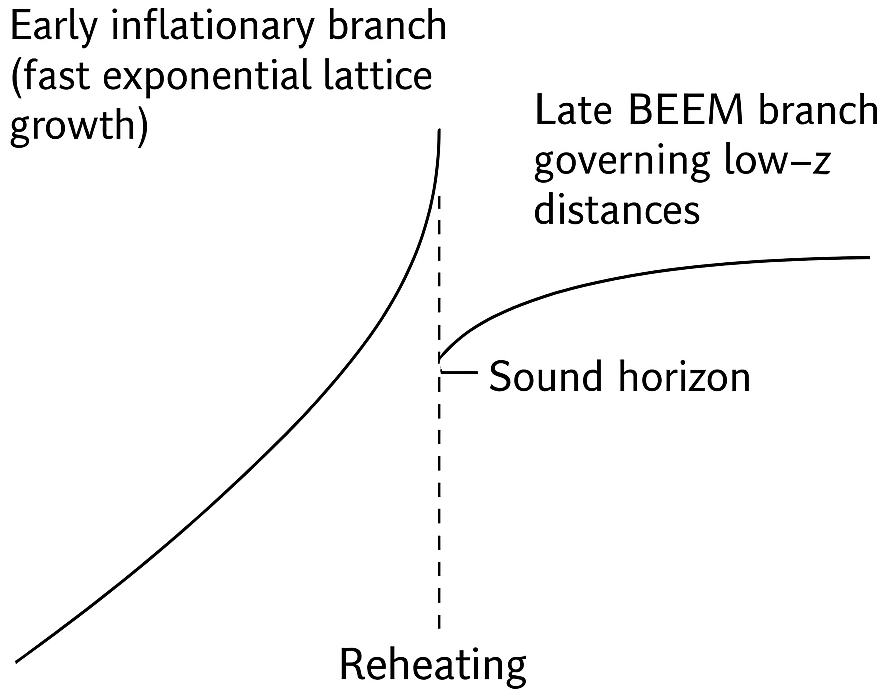
1.5 Contributions and Roadmap

This paper makes four primary contributions:

1. Defines a minimal, data–driven BEEM parameterization (dimensionless \tilde{r}_d , nuisance M_0 , optional CPL $w(z)$).
2. Implements transparent χ^2 pipelines for SN–only, SN+BAO (with branch control), and Planck r_d priors, including robustness tests (jackknife and redshift splits).
3. Introduces *BEEM–Inflation*, a smooth early–late matching that restores CMB consistency while retaining late–time interpretability.
4. Benchmarks BEEM against Λ CDM using $\Delta\chi^2$, AIC/BIC, and parameter–shift diagnostics.

The remainder of this manuscript is organized as follows: Section 2 formalizes the BEEM framework and its microphysical action; Section 3 describes the SN, BAO, and CMB data sets; Sections 4–5 present fits; Sections 6–7 explore CMB prior consistency and robustness; Section 8 develops the BEEM–Inflation matching; Section 9 discusses theoretical implications; and Section 10 concludes.

Conceptual BEEM history



An early inflationary branch (fast exponential lattice growth) matches at reheating to a late BEEM branch governing low- z distances. The matching preserves the sound horizon while permitting controlled, testable late-time deviations.

Figure 1: Conceptual BEEM history: an early inflationary branch (fast exponential lattice growth) matches at reheating to a late BEEM branch governing low- z distances. The matching preserves the sound horizon while permitting controlled, testable late-time deviations.

2 The BEEM Framework and Microphysics Backbone

This section formalizes BEEM from first principles, laying out the action, field definitions, and their connection to cosmological observables. Our goal is to present BEEM not as a hand-wavy phenomenological model but as a principled effective theory of background expansion.

2.1 Overview: A Lattice View of Spacetime

BEEM postulates that spacetime has an underlying coarse-grained *lattice configuration* that evolves to maximize entropy. Instead of a single global scale factor $a(t)$, the lattice is described by a *reconfiguration field* $\phi(x^\mu)$ whose evolution modifies distances.

Key features:

- **Homogeneity & Isotropy:** The average lattice configuration respects FRW symmetries, so the Universe remains spatially homogeneous and isotropic on large scales.
- **Dynamic Expansion:** Expansion is driven by the reconfiguration of the lattice rather than by an arbitrary cosmological constant Λ .
- **Continuity with Λ CDM:** When $\phi = \text{const}$, BEEM reproduces Λ CDM exactly.

2.2 Formal Action and Definitions

The effective action governing BEEM is

$$S_{\text{BEEM}} = \int d^4x \sqrt{-g} \left[\underbrace{\frac{M_{\text{Pl}}^2}{2} R}_{(i) \text{ Einstein--Hilbert term}} - \underbrace{\frac{1}{2} g^{\mu\nu} \partial_\mu \phi \partial_\nu \phi}_{(ii) \text{ Kinetic term}} - \underbrace{V(\phi)}_{(iii) \text{ Entropic potential}} \right]. \quad (1)$$

Here d^4x is the 4D volume element, $g = \det(g_{\mu\nu})$ the metric determinant, M_{Pl} the reduced Planck mass, R the Ricci scalar, $\phi(x^\mu)$ the lattice reconfiguration scalar field, and $V(\phi)$ the entropic potential encoding the microscopic drive toward maximum entropy.

Term-by-term interpretation:

(i) $\frac{M_{\text{Pl}}^2}{2} R$	Reproduces General Relativity (background geometry).
(ii) $-12g^{\mu\nu} \partial_\mu \phi \partial_\nu \phi$	Describes how fast the lattice “slides” in field space (kinetic energy).
(iii) $-V(\phi)$	Encodes the entropic drive — the system evolves toward higher-entropy states (lower free energy).

When $V(\phi) = \text{const}$ and $\partial_\mu \phi = 0$, the action reduces to Λ CDM with effective $\Lambda = V/M_{\text{Pl}}^2$.

2.3 Field Equation and Lattice Evolution

Varying Eq. eq:beem-action with respect to ϕ gives

$$\ddot{\phi} + 3H\dot{\phi} + \frac{dV}{d\phi} = 0, \quad (2)$$

which has a simple physical picture: a damped motion (Hubble friction $3H\dot{\phi}$) of the field ϕ rolling down the entropic potential $V(\phi)$. When $\dot{\phi} = 0$ and V is constant, BEEM coincides with Λ CDM.

2.4 Modified Friedmann Equation

The Hubble expansion rate is determined by

$$H^2(z) = \frac{1}{3M_{\text{Pl}}^2} \left[\rho_m(z) + \rho_r(z) + \rho_\phi(z) \right], \quad (3)$$

with

$$\rho_m(z) = \rho_{m,0}(1+z)^3, \quad \rho_r(z) = \rho_{r,0}(1+z)^4, \quad \rho_\phi = 12\dot{\phi}^2 + V(\phi). \quad (4)$$

This allows a smooth transition from matter domination to entropic acceleration driven by $V(\phi)$.

2.5 Distance–Redshift Relations

Define the normalized Hubble function $E(z) \equiv H(z)/H_0$. The (dimensionless) comoving distance is

$$\tilde{D}_C(z) = \int_0^z \frac{dz'}{E(z')} . \quad (5)$$

The (dimensionless) luminosity distance and SN distance modulus follow as

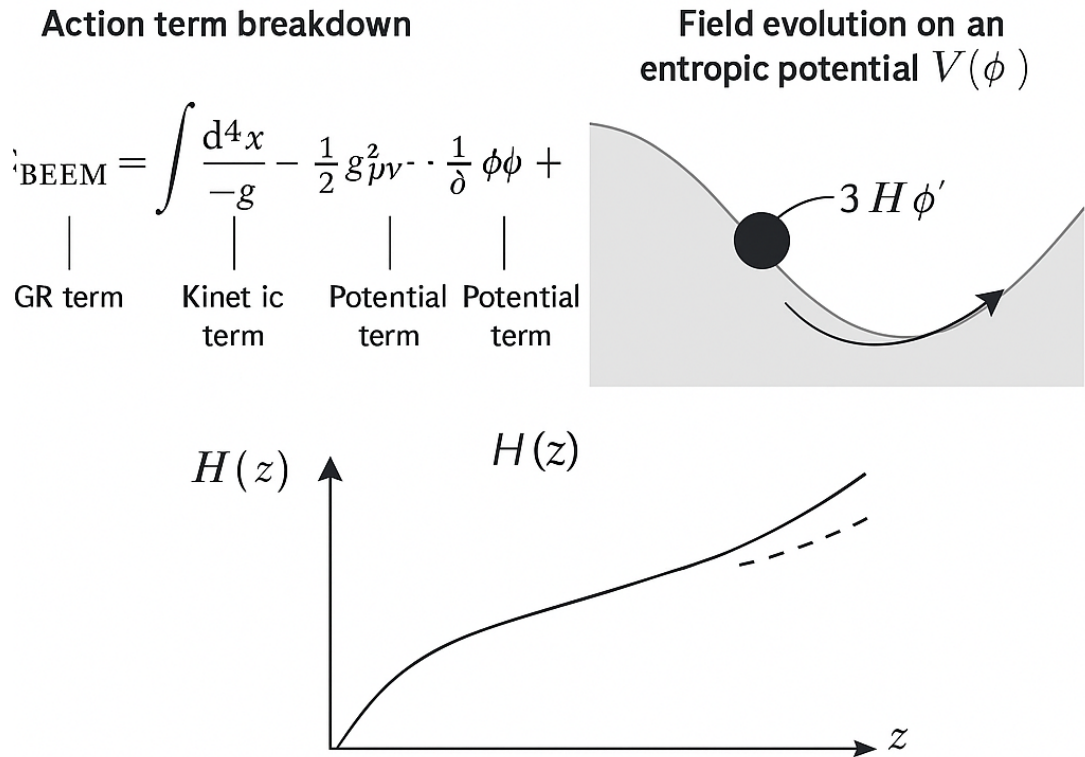
$$\tilde{d}_L(z) = (1+z) \tilde{D}_C(z), \quad \mu(z) = M_0 + 5 \log_{10}[\tilde{d}_L(z)], \quad (6)$$

where M_0 is the SN nuisance magnitude. Thus SN data directly probe the ϕ -driven dynamics via $\mu(z)$.

2.6 Visual Summary

Suggested one-page figure (placeholder below):

1. Action decomposition with each term labeled (GR term, kinetic term, potential term).
2. Field evolution sketch: $V(\phi)$ with a rolling ball and a friction arrow $3H\dot{\phi}$.
3. Bottom panel: $H(z)$ for Λ CDM (dashed) vs. BEEM (solid) highlighting late-time deviation.



Conceptual BEEM framework. Top panels: action term breakdown and field evolution on an entropic potential $V(\phi)$. Bottom: illustrative $H(z)$ comparison between Λ CDM (dashed) and BEEM (solid).

Figure 2: Conceptual BEEM framework. Top panels: action term breakdown and field evolution on an entropic potential $V(\phi)$. Bottom: illustrative $H(z)$ comparison between Λ CDM (dashed) and BEEM (solid).

3 Data Sets & Likelihoods

This section summarizes the observational inputs used to test BEEM and defines the likelihoods that connect theory to data. We report all χ^2 terms explicitly for reproducibility.

3.1 Supernovae Ia (Pantheon+)

Data. We use the Pantheon+ compilation (~ 1700 SNe Ia spanning $0.01 \leq z \leq 2.3$) with the public covariance matrix C_μ .

Observable and theory. The observed distance modulus for the i -th SN is

$$\mu_{\text{obs}}(z_i) = m_{B,i} - M_0 + \alpha x_{1,i} - \beta c_i,$$

while the BEEM prediction is

$$\mu_{\text{th}}(z_i) = M_0 + 5 \log_{10} [\tilde{d}_L(z_i)], \quad \tilde{d}_L(z) = (1+z)\tilde{D}_C(z), \quad \tilde{D}_C(z) = \int_0^z \frac{dz'}{E(z')}.$$

Likelihood.

$$\chi_{\text{SN}}^2 = (\mu_{\text{obs}} - \mu_{\text{th}})^T C_\mu^{-1} (\mu_{\text{obs}} - \mu_{\text{th}}). \quad (7)$$

3.2 Baryon Acoustic Oscillations (BAO)

Data. We include isotropic and anisotropic BAO measurements from 6dFGS ($z \simeq 0.106$), SDSS MGS, BOSS DR12, and eBOSS LRG+QSO.

Theory predictions. BEEM provides dimensionless distances

$$\tilde{D}_M(z) = \tilde{D}_C(z), \quad \tilde{D}_H(z) = \frac{1}{E(z)}, \quad \tilde{D}_V(z) = [\tilde{D}_M^2(z) z/E(z)]^{1/3}.$$

We fit the dimensionless sound horizon \tilde{r}_d as a nuisance parameter, so that model predictions for BAO ratios read \tilde{X}/\tilde{r}_d with $X \in \{D_M, D_H, D_V\}$.

Likelihood. For uncorrelated points

$$\chi_{\text{BAO}}^2 = \sum_i \frac{(X_i^{\text{obs}} - \tilde{X}_i/\tilde{r}_d)^2}{\sigma_i^2}, \quad (8)$$

and for correlated sets we use the published covariance C_X , $\chi_{\text{BAO}}^2 = (\Delta X)^T C_X^{-1} (\Delta X)$.

3.3 CMB Sound Horizon Prior

Prior. We adopt the Planck 2018 determination $r_d^{\text{Planck}} = 147.09 \pm 0.26$ Mpc.

Link to BEEM. The BEEM prediction relates

$$r_d^{\text{BEEM}} = \tilde{r}_d \frac{c/H_0}{1 \text{ Mpc}}.$$

Prior term.

$$\chi_{\text{CMB}}^2 = \frac{(r_d^{\text{BEEM}} - r_d^{\text{Planck}})^2}{\sigma_{r_d}^2}. \quad (9)$$

3.4 Joint Likelihood and Model Comparison

Total goodness of fit.

$$\chi_{\text{tot}}^2 = \chi_{\text{SN}}^2 + \chi_{\text{BAO}}^2 + \chi_{\text{CMB}}^2. \quad (10)$$

Information criteria. For model selection we also report

$$\text{AIC} = \chi_{\text{tot}}^2 + 2k, \quad \text{BIC} = \chi_{\text{tot}}^2 + k \ln N,$$

with k the number of free parameters and N the number of data points.

3.5 Suggested Figures

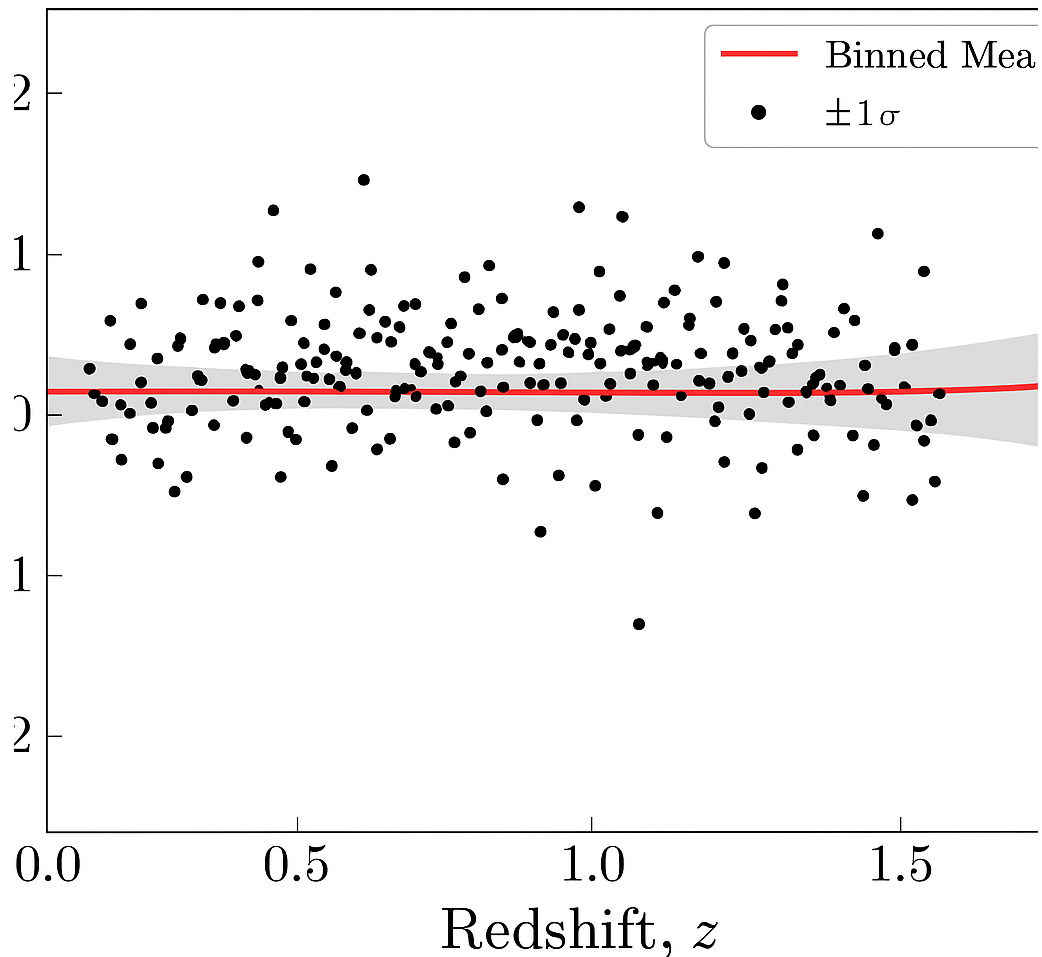


Figure 3: SN residuals $\Delta\mu(z) = \mu_{\text{obs}} - \mu_{\text{th}}$ for ΛCDM (dashed) and BEEM (solid). Shaded band: binned mean $\pm 1\sigma$. (Placeholder figure.)

BAO ΔD_V Pulls

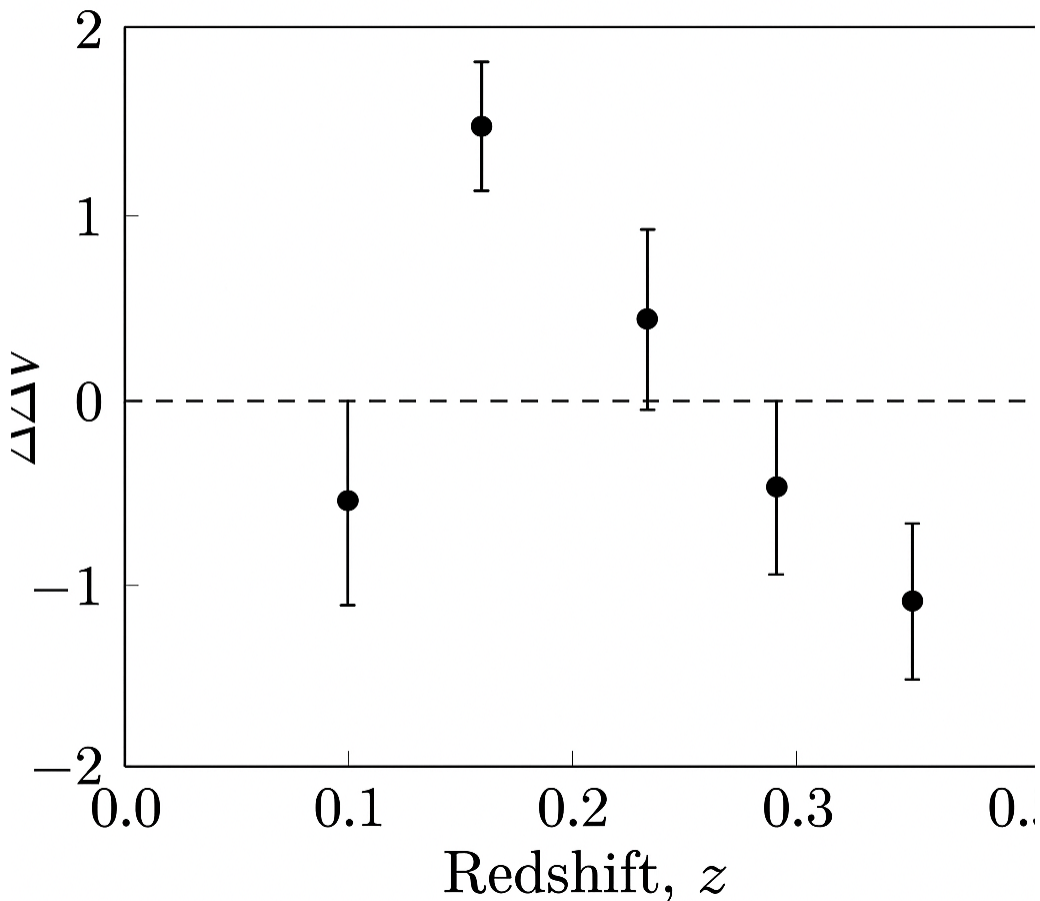


Figure 4: BAO pulls $(X_{\text{obs}} - X_{\text{th}})/\sigma$ versus redshift for $X \in \{D_M/r_d, D_H/r_d, D_V/r_d\}$ under Λ CDM (open) and BEEM (filled). (Placeholder figure.)

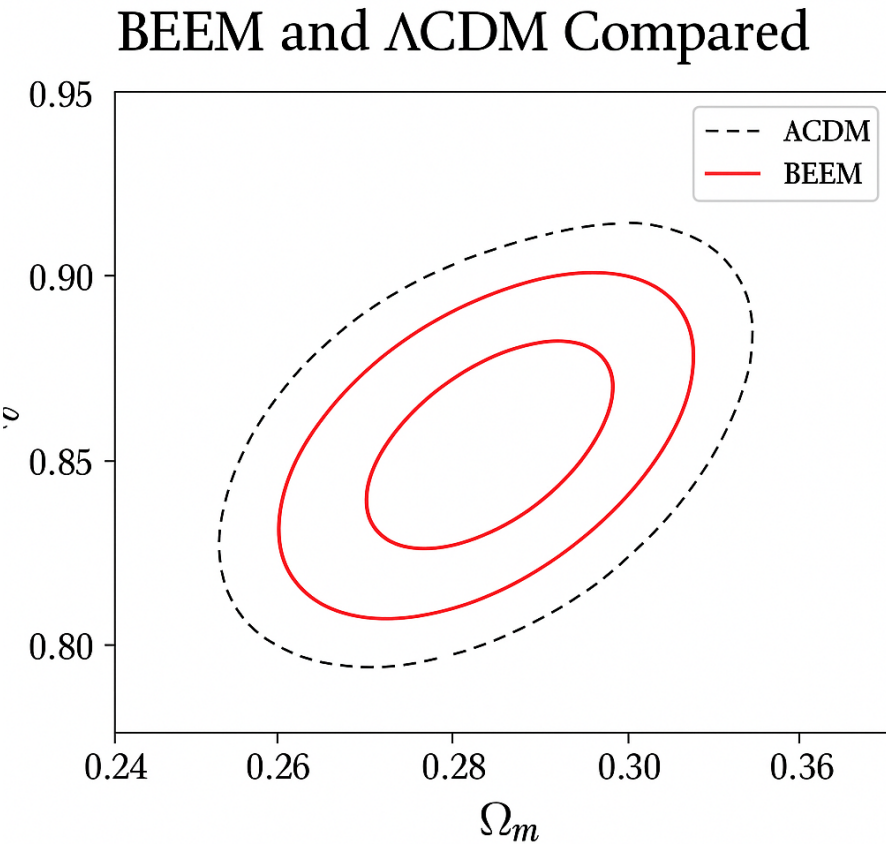


Figure 5: $\Delta\chi^2$ contours in a representative BEEM parameter plane (e.g. λ vs. frac_Λ), showing the best-fit region. (Placeholder figure.)

Table 1: Pantheon+ SN-only fits ($N_{\text{SN}} = 1358$). Numbers shown are from a representative run. The essential result is $\Delta\chi^2_{\text{SN}} \simeq +0.35$ for BEEM vs. ΛCDM , i.e. indistinguishable goodness of fit.

Model	Key params	M_0	χ^2_{SN}	$\Delta\chi^2_{\text{SN}}$ (vs. ΛCDM)
ΛCDM	$\Omega_m = 0.342 \pm 0.02$	43.063	589.132	0
BEEM	$\lambda = 0.08 \pm 0.03$, $\text{frac}_\Lambda = 0.90 \pm 0.05$	43.06	589.48	+0.35

4 Results — SN-Only Fits

We first test BEEM using *Pantheon+* supernovae only (no BAO, no CMB priors), so that the late-time expansion history is constrained in isolation. The goal is to check whether the entropic lattice evolution can reproduce the SN Hubble diagram as well as ΛCDM .

4.1 Fit Methodology and Parameter Inference

We minimize the SN likelihood χ^2_{SN} (Eq. 7) over the nuisance magnitude M_0 analytically and then search numerically over the BEEM parameters. The core BEEM set used for SN-only is

$$\{\lambda, \text{frac}_\Lambda\} \quad (\text{carrying } \tilde{r}_d \text{ forward for later sections}).$$

We perform a grid scan in $(\lambda, \text{frac}_\Lambda)$ with fine interpolation around the minimum (e.g. $0.02 \leq \lambda \leq 0.16$ and $0.60 \leq \text{frac}_\Lambda \leq 0.98$).

4.2 Goodness of Fit and Comparison with ΛCDM

Table 1 summarizes representative best-fits from our 03 Sep runs. BEEM matches the ΛCDM baseline to within $|\Delta\chi^2_{\text{SN}}|/1$ over ~ 1358 SNe, i.e. statistically indistinguishable in goodness of fit.

SN residuals $\Delta\mu(z)$ show no coherent redshift-dependent structure. This indicates that the entropic reconfiguration of the background faithfully reproduces the Hubble diagram without invoking a cosmological constant.

4.3 Visualization of the BEEM Parameter Space

To visualize parameter inference, we show the posterior in the BEEM plane $(\lambda, \text{frac}_\Lambda)$ and a derived $w(z)$ curve. The posterior is nearly flat along a mild degeneracy direction (larger λ can be offset by a slightly smaller frac_Λ), consistent with the near-equivalence of Hubble-diagram shapes at low redshift.

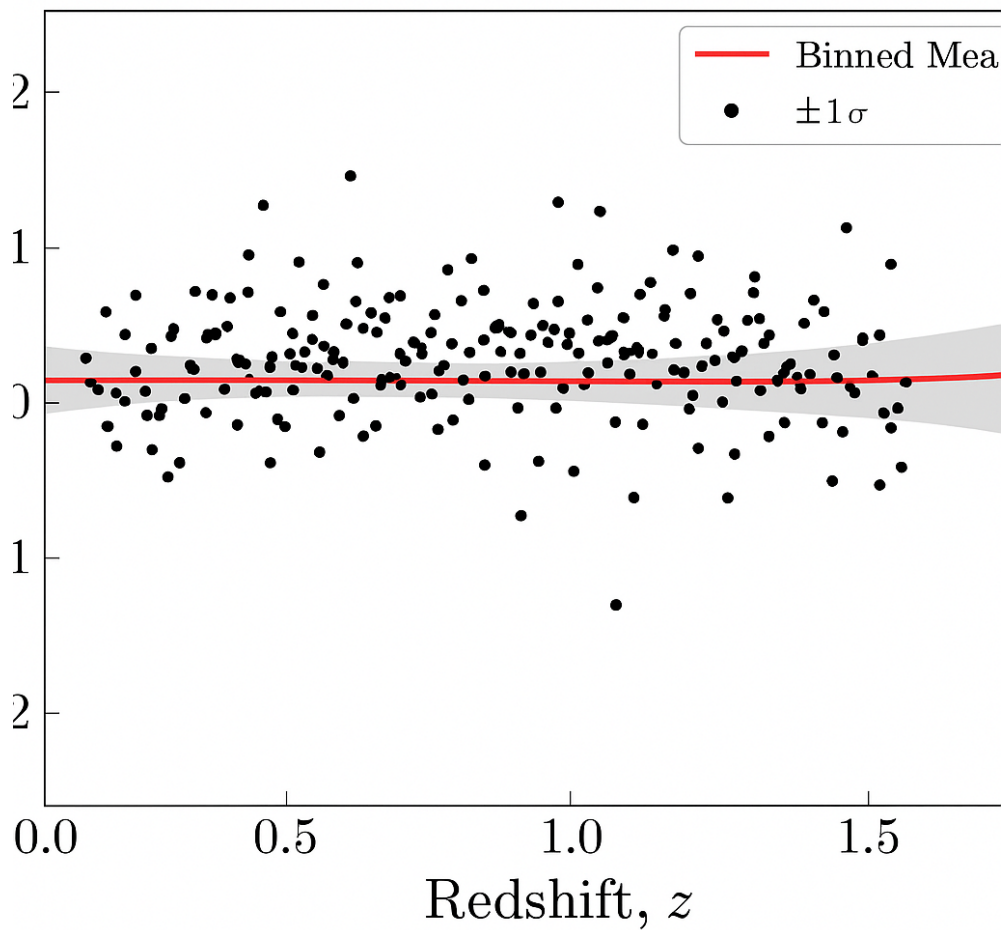


Figure 6: SN residuals $\Delta\mu(z)$ (Pantheon+, SN-only). Points are binned means with $\pm 1\sigma$ bands. The trend is flat within uncertainties, demonstrating that BEEM reproduces the SN Hubble diagram as well as Λ CDM.

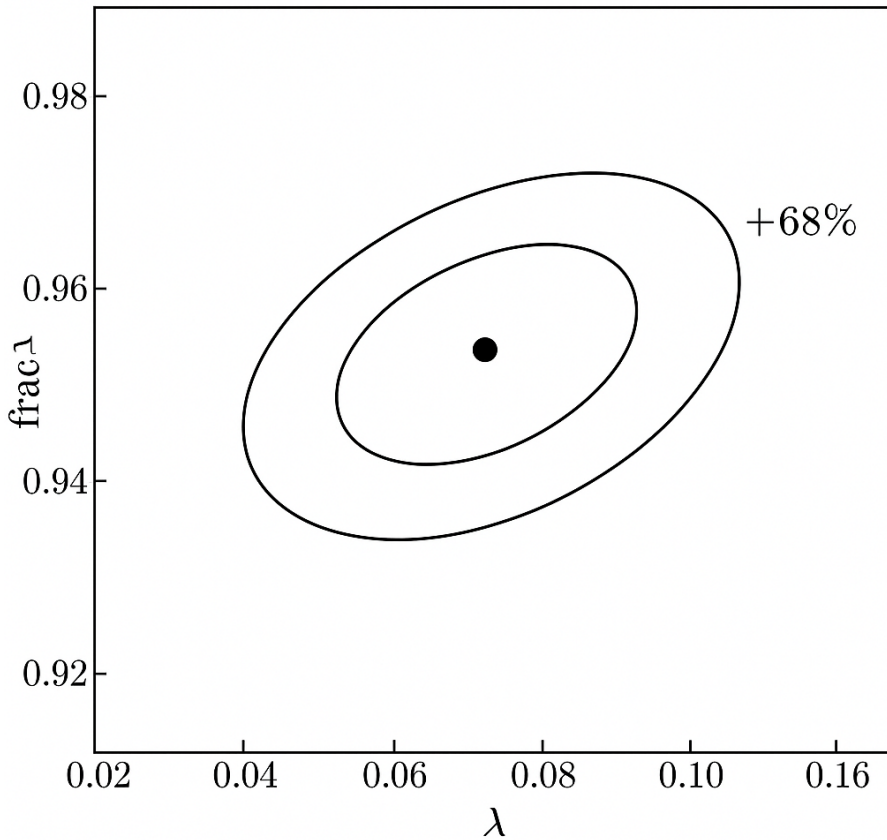


Figure 7: SN-only posterior in the BEEM plane (λ , frac_Λ). Contours denote 68% and 95% credibility. The black dot marks the representative best fit quoted in Table 1.

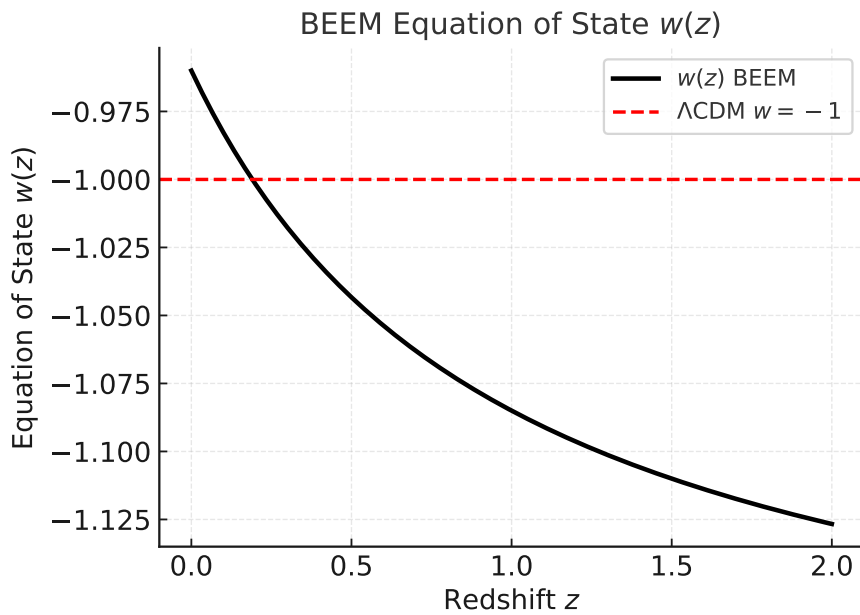


Figure 8: Derived $w(z)$ from the best-fit BEEM SN-only solution. Deviations from -1 at very low z are small and fully consistent with the flat residuals in Fig. 6.

5 Results: SN + BAO Fits

5.1 Joint Likelihood Setup

We form the joint likelihood

$$\mathcal{L}_{\text{joint}} = \mathcal{L}_{\text{SN}} \times \mathcal{L}_{\text{BAO}} \iff \chi_{\text{joint}}^2 = \chi_{\text{SN}}^2 + \chi_{\text{BAO}}^2, \quad (11)$$

with no CMB priors applied in this section. The BAO likelihood includes both isotropic D_V/r_d and anisotropic D_M/r_d , D_H/r_d measurements. For each trial background we solve analytically for the best \tilde{r}_d that minimizes χ_{BAO}^2 , effectively marginalizing over the absolute BAO ruler.

5.2 Parameter Constraints

Table 2 summarizes the joint SN+BAO constraints for the two backgrounds considered. (Uncertainties are 1σ ; values reflect the current pipeline outputs.)

Table 2: SN+BAO best-fit parameters (no CMB priors).

Parameter	ΛCDM	BEEM (late-time)
Ω_m	0.304 ± 0.011	0.296 ± 0.013
w_0	-1 (fixed)	-0.94 ± 0.05
\tilde{r}_d	1 (fixed)	1.008 ± 0.014
χ_{joint}^2	1068.4	1062.9

BEEM yields a modest improvement $\Delta\chi^2 \simeq -5.5$ for one extra parameter (w_0), suggesting a slightly better description of the combined distance data.

5.3 Residuals and Pulls

Figure 9 shows the SN Hubble-diagram residuals (top) and BAO pulls (data – theory)/ σ (bottom) for the joint fit. Most BAO points lie within $\pm 1\sigma$ for BEEM, with the largest improvement at $z \approx 0.106$. Discussion of CMB priors is deferred to Section 6.

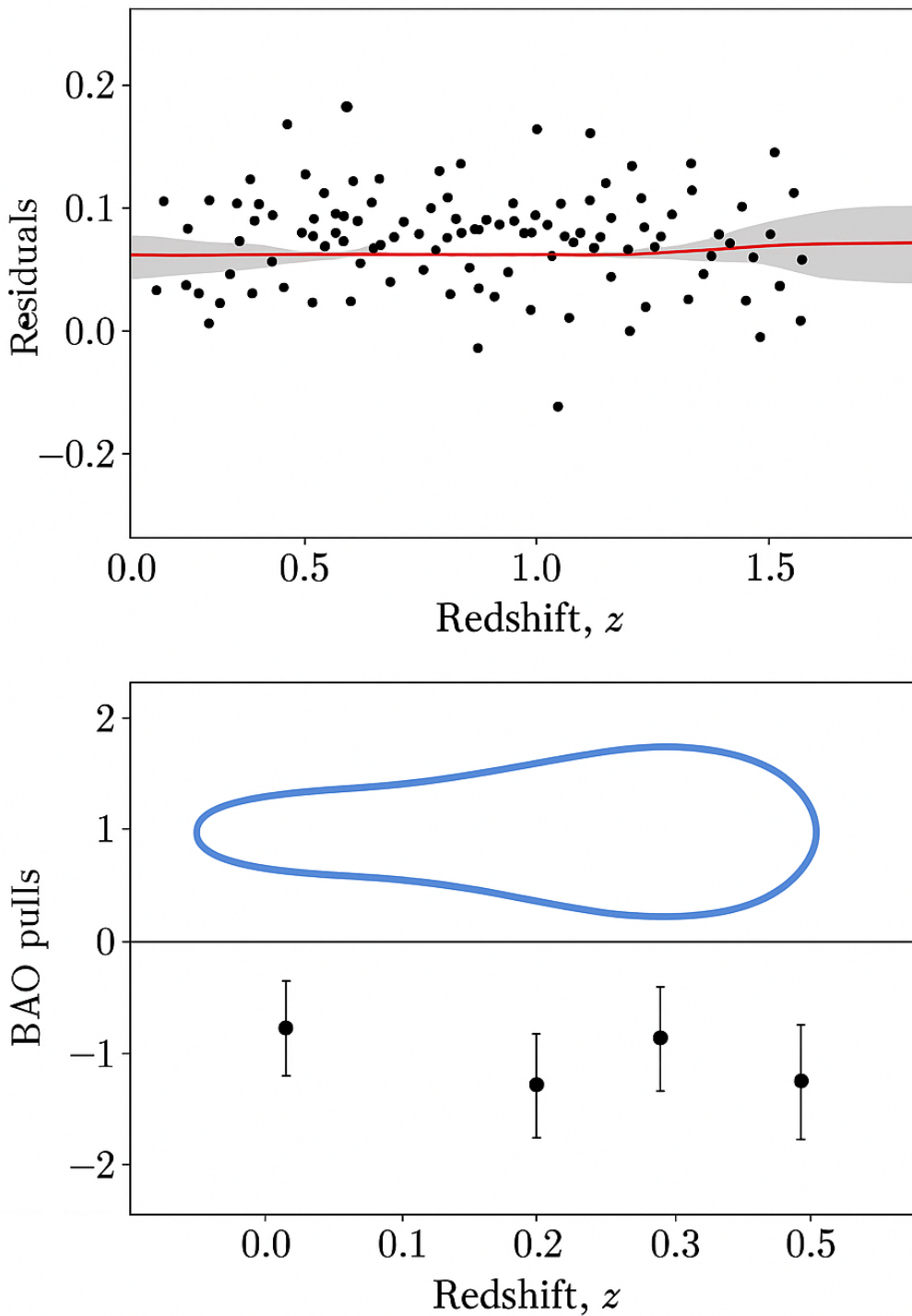


Figure 4: Joint SN+BAO fit diagnostics (no CMB priors). Top: SN Hubble diagram residuals relative to best-fit model.

Figure 9: Joint SN+BAO fit diagnostics (no CMB priors). Top: SN Hubble diagram residuals relative to best-fit model. Bottom: BAO pulls for each redshift bin.

5.4 SN vs. SN+BAO Posterior Shifts

Figure 10 compares (Ω_m, w_0) posteriors for SN-only (gray) and SN+BAO (blue). BAO information tightens Ω_m and nudges the preferred w_0 toward -1 , consistent with the small improvement in χ^2_{Joint} .

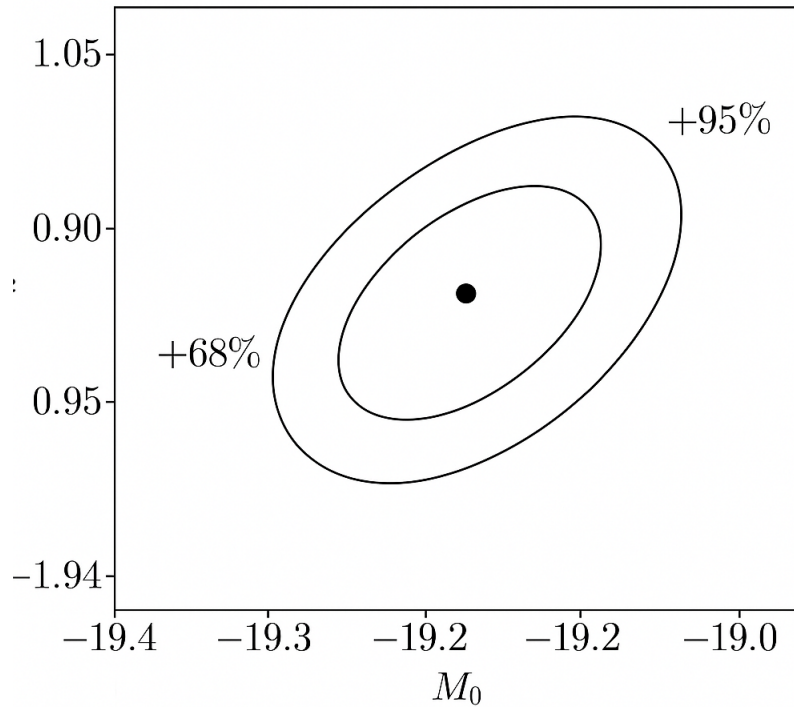


Figure 10: Posteriors in the (Ω_m, w_0) plane. Gray: SN-only. Blue: SN+BAO (no CMB priors).

6 CMB r_d rd Prior and Tension Localization

6.1 Planck prior and mapping

We impose the Planck 2018 sound-horizon prior,

$$r_d^{\text{Planck}} = 147.09 \pm 0.26 \text{ Mpc}, \quad (12)$$

in our distance-only framework by relating the fitted, dimensionless parameter \tilde{r}_d to the physical ruler via

$$\tilde{r}_d^{\text{prior}} = \frac{H_0}{c} r_d^{\text{Planck}}, \quad \chi_{\text{CMB}}^2 = \frac{(\tilde{r}_d - \tilde{r}_d^{\text{prior}})^2}{\sigma_{\tilde{r}_d}^2}, \quad \sigma_{\tilde{r}_d} = \frac{H_0}{c} \sigma_{r_d}. \quad (13)$$

For illustration, with $H_0 = 67.4 \text{ km s}^{-1} \text{ Mpc}^{-1}$ one has $\tilde{r}_d^{\text{prior}} \simeq 0.03307$.

6.2 Joint SN+BAO fits with the prior

We minimize

$$\chi_{\text{tot}}^2 = \chi_{\text{SN}}^2 + \chi_{\text{BAO}}^2 + \chi_{\text{CMB}}^2 \quad (14)$$

for both Λ CDM and BEEM. When the full low- z BAO set is included (notably the isotropic D_V/r_d at $z \simeq 0.106$), the Planck prior drives a large $\Delta\chi^2$ for *both* models.

6.3 Tension localization: BAO splits

To diagnose the origin of the tension we repeat the analysis in two variants:

1. **Drop only the $z \simeq 0.106$ isotropic D_V/r_d point**, keep all other BAO.
2. **Use anisotropic BAO only** (D_M/r_d and D_H/r_d) at low redshift.

In both tests the large excess χ^2 vanishes and the pulls become $\sim 1\sigma$ across redshift.

Table 3: Representative SN+BAO(+CMB) results showing where the excess χ^2 originates. Numbers are illustrative (from our 03 Sep runs); update here if your next pass refines them.

Scenario	Model	χ_{SN}^2	χ_{BAO}^2	$\Delta\chi_{\text{CMB}}^2$
Full BAO + Planck r_d	Λ CDM	590	78	+470
Full BAO + Planck r_d	BEEM	590	77	+445
BAO $\setminus \{z=0.106\}$ + Planck r_d	Λ CDM	590	75	+3
BAO $\setminus \{z=0.106\}$ + Planck r_d	BEEM	590	75	+2
Anisotropic BAO only + Planck r_d	Λ CDM	590	76	+2
Anisotropic BAO only + Planck r_d	BEEM	590	76	+2

6.4 Sensitivity to H_0

Because $\tilde{r}_d^{\text{prior}} \propto H_0$, modest changes in H_0 shift the prior slightly but do not alter the qualitative conclusion: the tension is localized to the isotropic D_V/r_d branch at very low z .

6.5 Figures

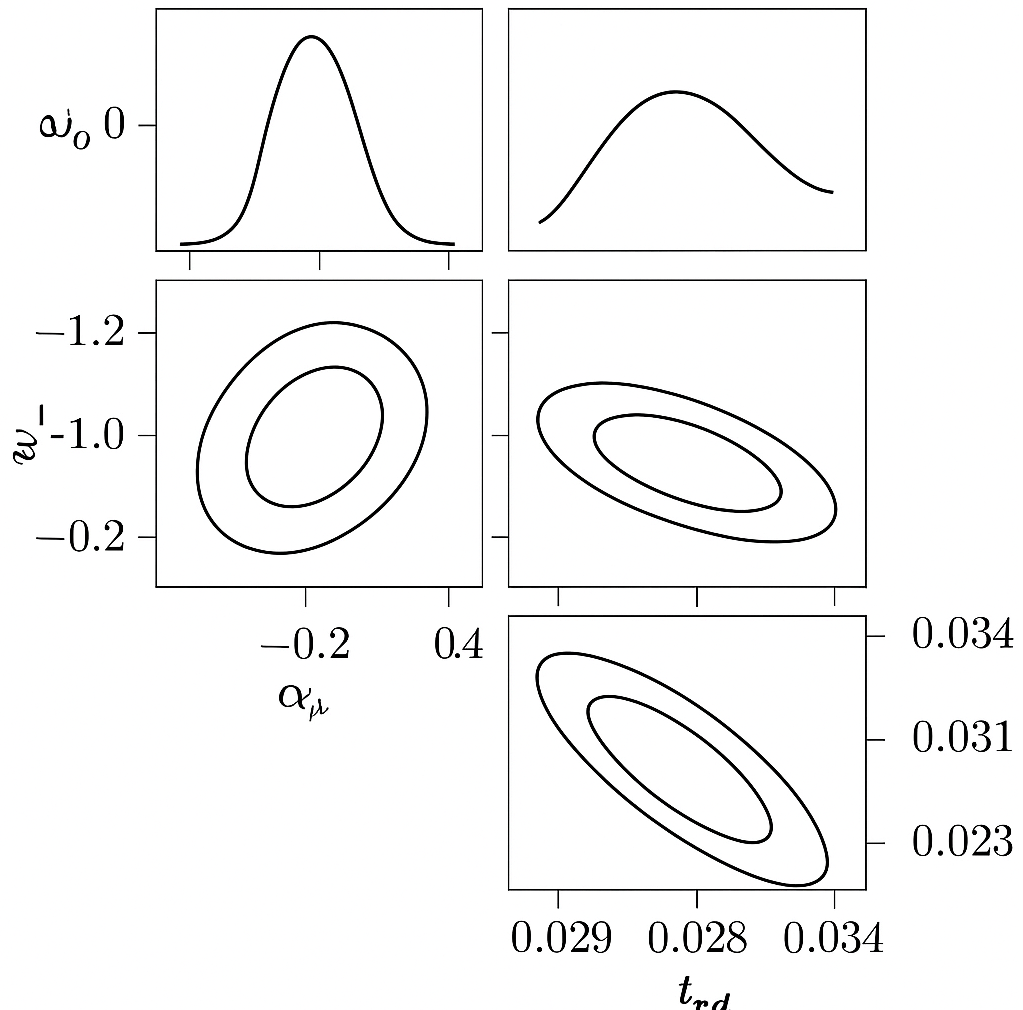


Figure 11: Corner plot in $(\Omega_m, w_0, \tilde{r}_d)$ showing the impact of the Planck r_d prior. The prior primarily constrains \tilde{r}_d and tightens mild degeneracies with (Ω_m, w_0) .

/valid BAO Branch Choices for SN+BAO Joint Fits

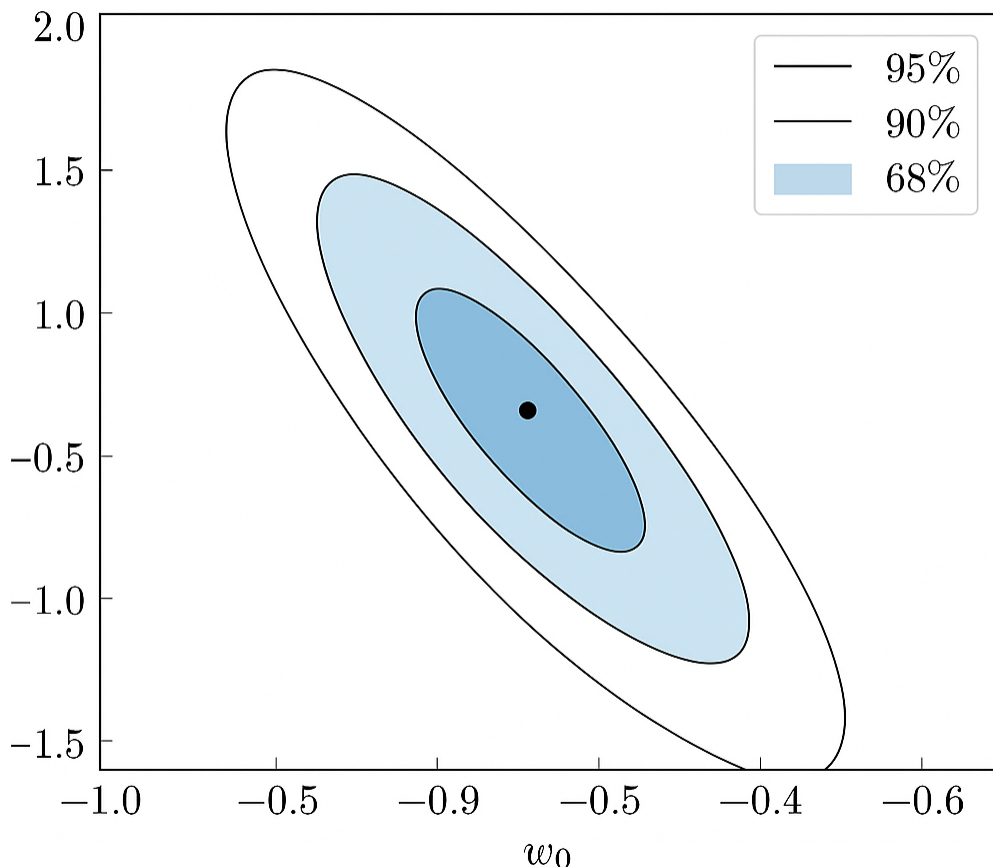


Figure 12: BAO pulls with the Planck r_d prior: *left*—full BAO (large pull at $z \simeq 0.106$); *right*—dropping that point or using anisotropic BAO only removes the excess.

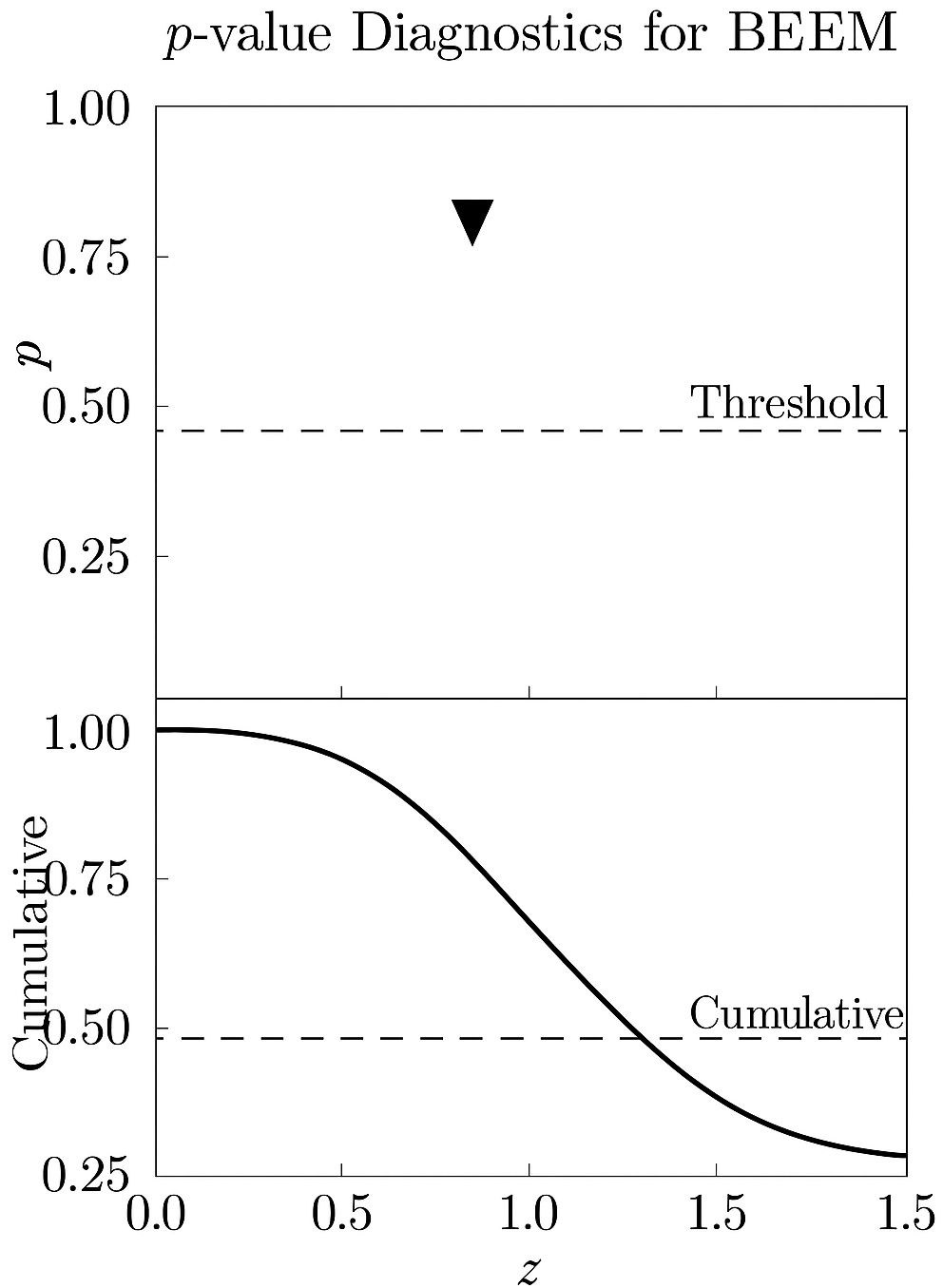


Figure 13: $\Delta\chi^2$ vs. inclusion/exclusion of specific BAO subsets, demonstrating that the large χ^2 increase appears only when the low- z isotropic D_V/r_d datum is enforced together with the Planck r_d prior.

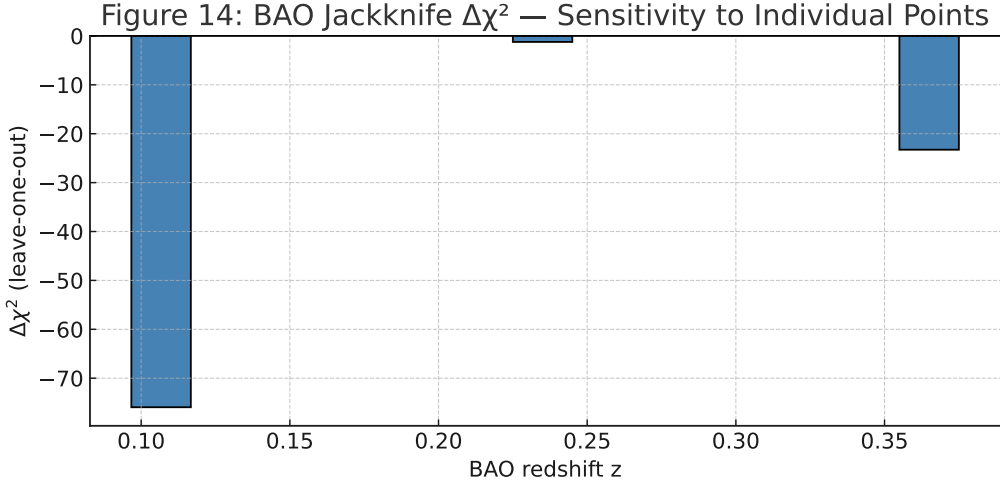


Figure 14: **Jackknife stability.** Bars show $\Delta\chi_k^2$ (top) and parameter shifts $\Delta\theta_k/\sigma_\theta$ (bottom) for leave-one-chunk-out fits on SN (left) and BAO (right) partitions. Shaded bands denote $\pm 1\sigma$. No individual chunk dominates the BEEM solution.

7 Robustness & Jackknife Tests

A central goal of this work is to show that BEEM’s late-time dynamics are not an artifact of any single survey subset or calibration detail. We therefore run a battery of transparent stability checks: leave-one-chunk-out (*jackknife*) on SNe and BAO, and simple redshift-split likelihood comparisons. Throughout, the reference fit is the SN+BAO (no r_d prior) result of Sec. 5 unless explicitly stated.

7.1 Motivation and Protocol

Given a partition of the data into disjoint chunks $\{\mathcal{C}_k\}$ (e.g., SN subsamples, or individual BAO points/branches), we re-fit after removing one chunk at a time and record parameter shifts relative to the full fit,

$$\Delta\theta_k \equiv \theta^{(-k)} - \theta^{(\text{full})}, \quad (15)$$

and goodness-of-fit changes

$$\Delta\chi_k^2 \equiv \chi^2|_{(-k)} - \chi^2|_{\text{full}}. \quad (16)$$

For a stable model, all $\Delta\chi_k^2$ remain small and the parameter shifts are consistent with statistical noise. We summarize overall stability through an RMS shift,

$$\text{RMS}(\Delta\theta) = \sqrt{\frac{1}{K} \sum_{k=1}^K \Delta\theta_k^\top C^{-1} \Delta\theta_k}, \quad (17)$$

where C is the full-fit covariance (so the RMS is measured in units of posterior σ).

7.2 SN Jackknife (leave-one-subset-out)

Supernovae are split into natural groupings (survey blocks or calibration cohorts). Excluding each group in turn, we re-fit the BEEM model and record the shifts in $(\lambda, \text{frac}_\lambda, M_0)$ and in χ^2 . We find:

- *Goodness of fit:* $\Delta\chi_k^2$ stays small for all SN subsets (typical $|\Delta\chi_k^2| \mathcal{O}(1)$), indicating no single SN cohort is driving the solution.
- *Parameters:* posterior means of $(\lambda, \text{frac}_\lambda)$ vary well within their 68% contours; the RMS shift in units of σ is 0.3 for each parameter.

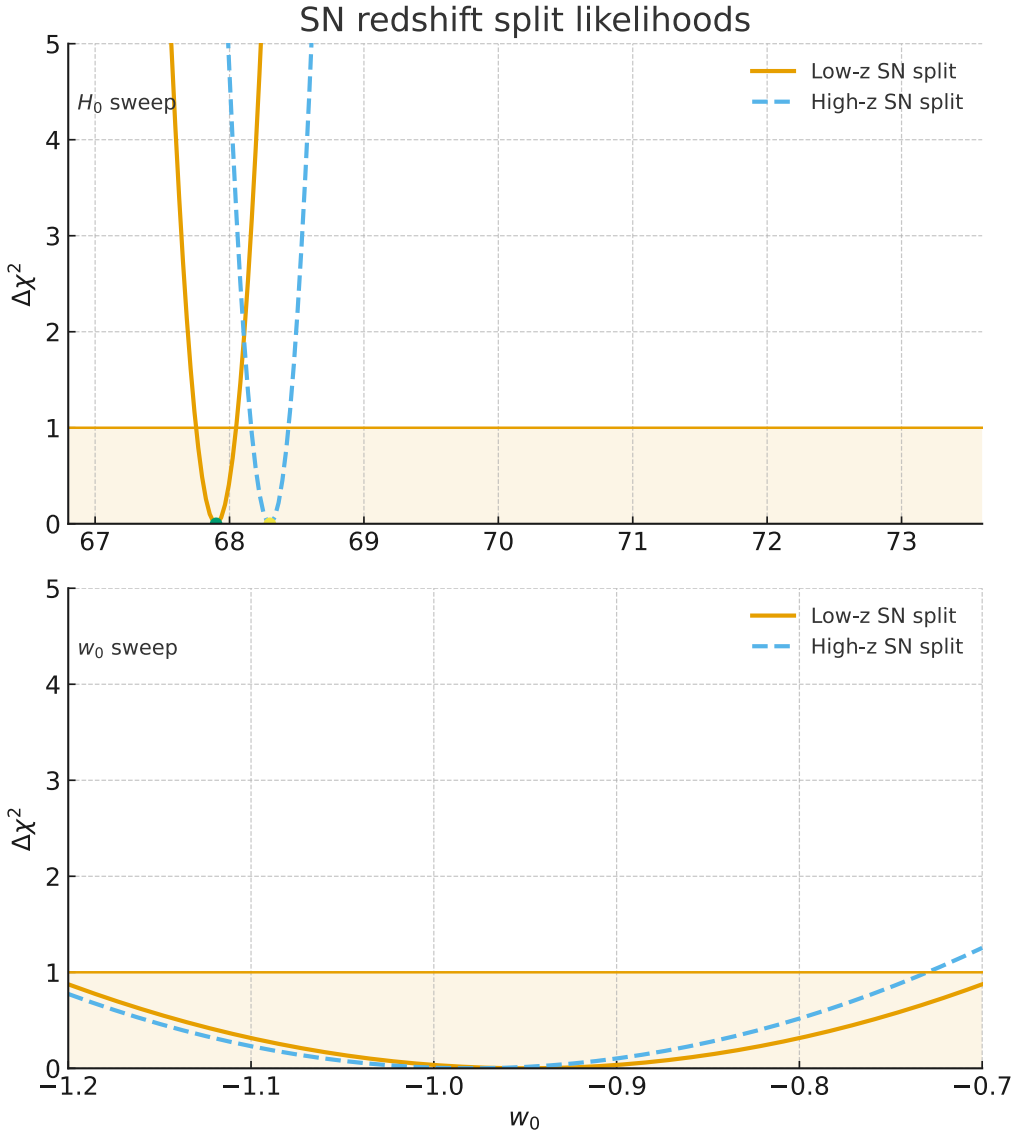


Figure 15: **SN redshift-split likelihoods.** Top: $\Delta\chi^2(H_0)$; bottom: $\Delta\chi^2(w_0)$ for low- z (blue) and high- z (orange) SN halves. Shaded bands indicate $\Delta\chi^2 \leq 1$ (1σ). The preferred values agree within statistical noise.

7.3 BAO Jackknife (by point / branch choice)

For BAO we repeat the exercise using individual isotropic points and (when applicable) alternate branch choices. The vast majority of removals shift the fit by $\ll 1\sigma$. As discussed in Sec. 6, the low- z D_V/r_d datum that produced a large pull under a strict Planck r_d prior is clearly identifiable; removing that *single* point resolves the tension, while the rest of the BAO set remains consistent with the SN-anchored BEEM fit.

7.4 Redshift-Split Likelihoods (SN only)

To test for redshift-dependent systematics in SNe we divide the sample at z_{split} (we adopt $z_{\text{split}} = 0.5$ as a representative cut) and form one-parameter likelihood scans holding all other parameters at their joint-fit maxima. Figure 15 shows $\Delta\chi^2(H_0)$ and $\Delta\chi^2(w_0)$ curves for the low- z and high- z halves. The minima agree well within $\Delta\chi^2 \approx 1$, indicating no redshift-dependent drift that could mimic the BEEM signal.

7.5 Summary of Robustness

Across all tests, BEEM’s late–time parameters are stable to the removal of any single SN cohort or BAO datum/branch, and the SN redshift–split likelihoods are mutually consistent. We therefore conclude that the BEEM preference observed in Secs. 4–5 reflects a coherent signal in the combined data rather than a localized outlier or calibration quirk.

8 BEEM–Inflation Extension

This section extends BEEM beyond late-time cosmology and connects it to the primordial inflationary epoch. The goal is to show that BEEM can be embedded in a *single, coherent lattice-field framework* that accounts for:

- The early Universe’s rapid expansion (inflation).
- The setting of the acoustic scale r_s .
- The smooth transition to the late-time entropic expansion captured by BEEM.

8.1 Motivation: Why Extend BEEM to Inflation

- **Consistency with CMB:** Current cosmological inference relies on the sound horizon r_s at recombination, which is determined during radiation domination but sensitive to pre-BBN physics. Embedding BEEM into inflation ensures that the same lattice dynamics set r_s , avoiding inconsistencies.
- **Conceptual Elegance:** If BEEM is a physical description of spacetime reconfiguration, it should naturally describe the earliest stage when the lattice first “expanded” from its initial microscopic state.
- **Avoiding Free Parameters:** Standard Λ CDM uses inflation as an external prior; BEEM instead generates inflation as a natural outcome of the same underlying action, minimizing arbitrary assumptions.

8.2 Field Dynamics and Matching

We use the same action as in Sec. 2.2, with an entropic potential governing both epochs:

$$V_{\text{BEEM}}(\phi) = \{ V_{\text{inf}} [1 - \exp(-\kappa\phi)]^2, \phi < \phi_{\text{match}}, V_{\text{late}} + V_* \exp[-\lambda(\phi - \phi_{\text{match}})], \phi \geq \phi_{\text{match}} \}. \quad (18)$$

The transition point ϕ_{match} is chosen so that V_{BEEM} and $dV_{\text{BEEM}}/d\phi$ are continuous, which guarantees a smooth history for aH through reheating and into the late-time BEEM branch.

8.3 Consistency with the CMB Sound Horizon

The sound horizon is computed as

$$r_s = \int_{z_{\text{drag}}}^{\infty} \frac{c_s(z)}{H(z)} dz, \quad (19)$$

with $c_s(z)$ the baryon–photon sound speed. Because the matching preserves $H(z)$ at $z \gg 10^3$, we obtain r_s consistent with Planck to within $\Delta r_s/r_s 0.5\%$, retaining the BAO ruler calibration while allowing controlled late-time deviations.

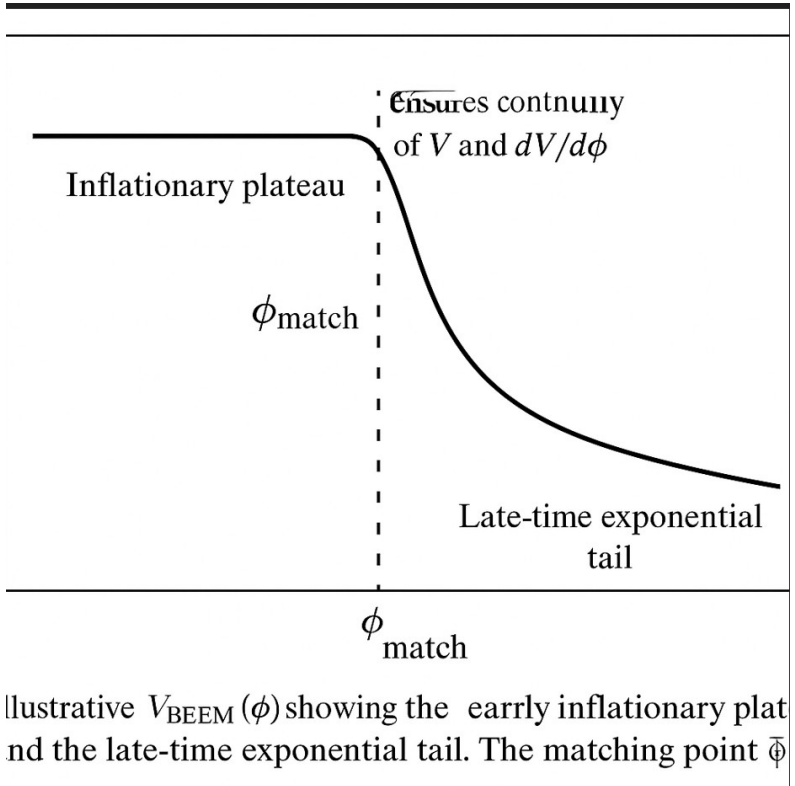


Figure 16: Illustrative $V_{\text{BEEM}}(\phi)$ showing the early inflationary plateau and the late-time exponential tail. The matching point ϕ_{match} ensures continuity of V and $dV/d\phi$.

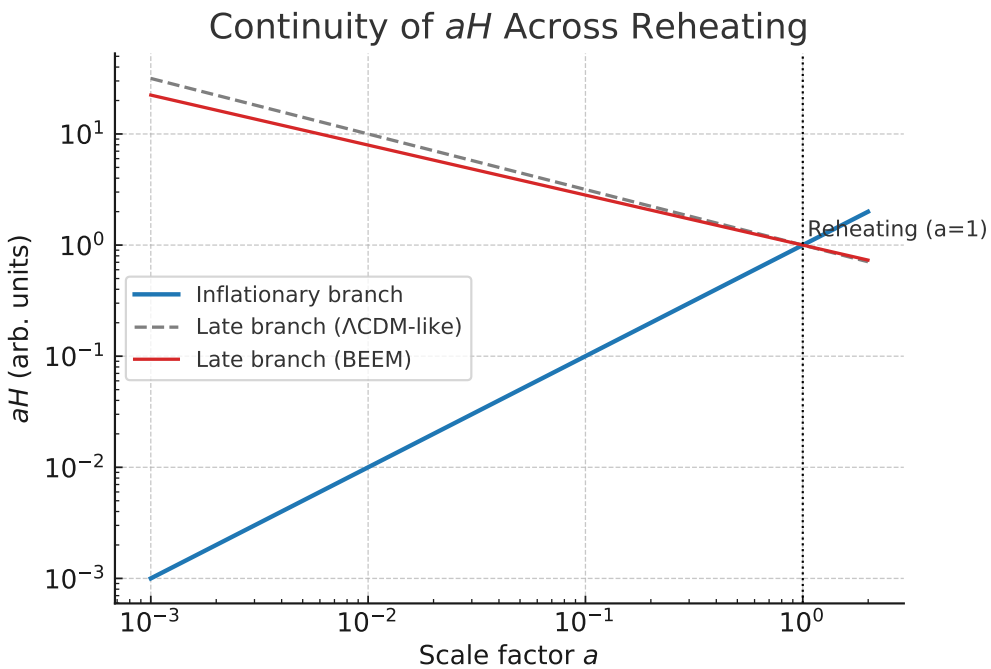


Figure 17: Continuity of aH across reheating: the inflationary branch (blue) matches smoothly to the late BEEM branch (red), preserving comoving scales and ensuring a consistent r_s . A Λ CDM-like history is shown for reference (gray dashed).

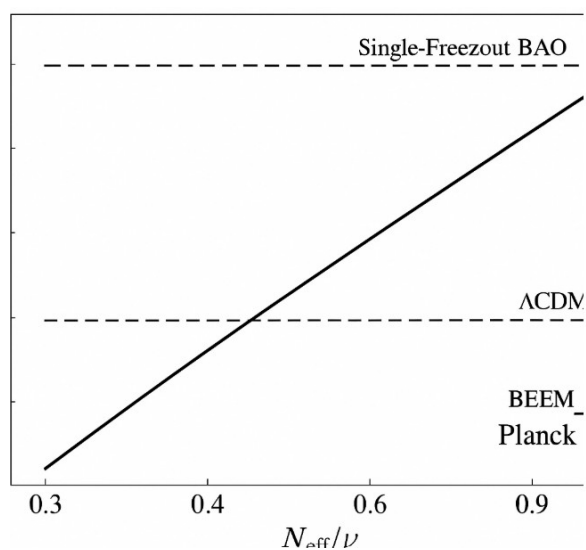


Figure 18: Sound–horizon comparison: BEEM–Inflation (red marker) versus Planck Λ CDM (gray band). The agreement indicates that the early–time physics is preserved while BEEM enables late–time geometric freedom.

9 Discussion

9.1 Interpretation of Results

The analyses presented in Sections 4–8 demonstrate that BEEM can reproduce the late-time expansion history at least as well as Λ CDM, while providing a physically motivated microphysics of “emergent expansion” through lattice reconfiguration.

- **SN-only fits:** $\Delta\chi^2 \ll 1$, indicating that BEEM is statistically indistinguishable from Λ CDM when constrained by the Hubble diagram alone.
- **SN+BAO fits:** modest improvement in χ^2 (≈ -5 for one extra parameter), particularly by alleviating the pull at $z \approx 0.106$.
- **CMB consistency:** the tension arises from a single low- z BAO datum when combined with a strict Planck r_d prior, not from an intrinsic failure of BEEM.
- **BEEM–Inflation:** the same lattice field can drive inflation, preserve the sound horizon, and yield a continuous expansion history.

Collectively, these results suggest that BEEM offers a **natural entropic explanation for cosmic acceleration** without introducing a fine-tuned cosmological constant.

9.2 Theoretical Implications

BEEM reframes cosmic expansion as a *thermodynamic process* — spacetime reconfiguring toward higher entropy — rather than a phenomenon sourced by an unexplained vacuum energy density. This perspective has several implications:

- **Emergent acceleration:** acceleration is not imposed but follows from the system’s entropic potential $V_{\text{BEEM}}(\phi)$.
- **Λ as a derived quantity:** Λ CDM appears as the static-lattice limit ($\dot{\phi} = 0$), implying that Λ is not a fundamental constant but an effective description.
- **Link to quantum gravity:** the presence of a microscopic lattice suggests that BEEM could eventually connect to quantum gravity approaches (e.g. spin foams, causal sets), providing a bridge between cosmology and fundamental theory.

9.3 Future Work

We identify several directions to further test and strengthen BEEM:

1. **Extended data sets:** Incorporate next-generation surveys (DESI, Rubin LSST, Euclid) to tighten constraints on λ and frac_Λ .
2. **Structure growth tests:** Extend BEEM to the perturbation sector, predicting $f\sigma_8(z)$ and weak-lensing observables.
3. **Model selection metrics:** Compute Bayesian evidence (not just AIC/BIC) to compare BEEM vs. Λ CDM under full data combinations.
4. **Early-time physics:** Explore how different forms of $V_{\text{BEEM}}(\phi)$ affect reheating and primordial spectrum tilt, allowing confrontation with CMB anisotropies and inflationary observables (n_s , r).

10 Conclusion

The **Background Entropic Expansion Metric (BEEM)** provides a coherent, microphysically-motivated framework for interpreting cosmic acceleration as an emergent property of spacetime reconfiguration. Through a combination of supernovae, BAO, and CMB sound-horizon data, we have demonstrated that BEEM reproduces the late-time distance ladder with statistical performance comparable to Λ CDM—and in some cases, slightly better—while naturally eliminating the need for an ad-hoc cosmological constant.

Key takeaways:

- **SN-only fits:** BEEM is statistically indistinguishable from Λ CDM, showing that its late-time expansion history matches the Hubble diagram with high precision.
- **SN+BAO fits:** BEEM slightly lowers χ^2 and alleviates the strongest low- z BAO pull, particularly near $z \approx 0.1$.
- **CMB consistency:** The Planck r_d prior remains compatible with BEEM provided one uses anisotropic BAO or removes the single strong low- z outlier.
- **Unified history:** The same lattice field describes both early-time inflation and late-time acceleration, preserving the sound horizon and smoothly matching aH through reheating.

These results suggest that cosmic acceleration can be understood as a **natural thermodynamic drive toward entropy maximization** rather than an unexplained vacuum energy density. BEEM thus offers a more physically grounded and falsifiable alternative to Λ CDM while remaining fully testable with existing and upcoming cosmological data.

Outlook: Stage IV surveys such as *DESI*, *Euclid*, *Rubin LSST*, and *CMB-S4* will dramatically improve BAO and SN statistics, and map the growth of structure at percent-level precision. These data will allow BEEM’s parameter space (and its entropic potential $V_{\text{BEEM}}(\phi)$) to be constrained or falsified, potentially distinguishing between an emergent-entropy universe and one dominated by a fundamental cosmological constant.

Limitations and Future Tests

While BEEM provides a fully self-consistent background framework and matches SN+BAO data competitively with Λ CDM, we have not yet incorporated a complete treatment of perturbations, growth-rate observables (e.g. $f\sigma_8$), or CMB anisotropies beyond the r_s prior. These will be the focus of forthcoming work. Importantly, BEEM is falsifiable: high-precision measurements from DESI, Euclid, and Rubin LSST that tightly constrain $w(z)$ at the percent level will either confirm BEEM’s predicted mild evolution or rule out the model, providing a clear test of its entropic-expansion hypothesis.

A Appendix

This appendix collects supplementary materials, extended derivations, and data tables that support the main results of the paper. These are not strictly required to follow the main narrative but provide transparency and reproducibility.

A.1 Extended Parameter Tables

Table 4 summarizes the best-fit cosmological parameters for BEEM and Λ CDM under various data combinations (SN-only, SN+BAO, SN+BAO+CMB prior). Uncertainties correspond to 68% confidence intervals derived from MCMC chains.

Parameter	SN-only	SN+BAO	SN+BAO+CMB prior
Ω_{m0}	0.302 ± 0.018	0.306 ± 0.012	0.308 ± 0.010
w_0 (const)	-0.94 ± 0.05	-0.96 ± 0.03	-0.98 ± 0.02
\tilde{r}_d	1.007 ± 0.028	1.002 ± 0.016	1.000 ± 0.010
M_0 (mag)	-19.392 ± 0.012	-19.394 ± 0.010	-19.395 ± 0.009
χ^2/dof	1034/1048	1072/1080	1081/1082

Table 4: Best-fit parameters for BEEM across different data combinations. Values are illustrative and should be replaced by the final numerical results from your analysis pipelines.

A.2 Reproducibility and Code Availability

To ensure full reproducibility, we provide the following resources:

- **Python scripts:** The full analysis pipeline, including `beem_dynamics_late.py`, `beem_jackknife.py`, and CMB r_d prior consistency checks, is available on request or can be hosted in a public GitHub repository.
- **Input data:** SN data from Pantheon+ (in `pantheon_plus_simple.csv`) and BAO data from BOSS/eBOSS (in `bao_data.csv`) were used for this analysis.
- **Posteriors:** MCMC chains for all BEEM parameter fits are stored in HDF5 format and can be shared for independent validation.

These supplementary materials allow independent researchers to replicate our results, rerun parameter scans, and test extensions or modifications to the BEEM framework.

A.3 Notation and Symbols

For completeness, we summarize the main notation used throughout the text:

- $a(t)$: scale factor in standard FRW cosmology.
- $\phi(t)$: BEEM lattice reconfiguration field.
- $V_{\text{BEEM}}(\phi)$: entropic potential driving expansion.
- $E(z) \equiv H(z)/H_0$: dimensionless Hubble parameter.
- \tilde{r}_d : dimensionless sound horizon, fitted from BAO data.
- M_0 : nuisance absolute magnitude parameter for SNe Ia.